Temperature-Dependent Influence of Molecular Orientation and Internal Stresses on the Deformation of Injection-Molded Polypropylene Parts

E. LAFRANCHE, J. PABIOT

Département des Polymères et Composites, Ecoles des Mines de Douai 941 rue Charles Bourseul, B.P 838, 59508 Douai Cedex, France

Received 28 May 1997; accepted 1 September 1997

ABSTRACT: Local orientation measures by infrared dichroism and thermal stress measures by dilatometric analysis of image (DAI) have made it possible to quantify the evolution of the structure versus the thickness of the injected plastic parts. The stiffness local properties on the one hand, and thermal expansion on the other hand, have then been established. Deformation measures made in temperature have pointed out its deformation induced by thermal stresses and that attributed to the gradient of molecular orientation and cristallinity of the polymer. A calculation of plastic part deformation constituted of elementary layers whose Young's modulus and coefficients of thermal expansion values have been previously evaluated, has enabled us to corroborate experimental results. © 1998 John Wiley & Sons, Inc. J Appl Polym Sci 68: 1661–1669, 1998

Key words: temperature dependence; molecular orientation; internal stress; injection-molded polypropylene parts

INTRODUCTION

The dimensional accuracy of an injected plastic part is directly linked to the structural homogeneity of the material. It is strongly influenced by shrinkages and residual stresses induced by the injection process. These stresses can be attributed to two main sources as described by Isayev et al.[1] The first stresses are due to flow stresses that arise from the filling stage of the mold but also, from the packing and postfilling stages[2] that produce the shear and normal stresses associated with elongational stresses. They increase the molecular orientation giving place to an increase of the entropy as indicated by Struik.[3] They have a low amplitude and they do not directly participate in the deformation on the plastic part, but they induce local anisotropies of the material properties as Young's modulus or thermal expansion that favor the load imbalance when shrinking. Their generation mechanism has been described by the Fountain flow,[4,5] which is easily shown by the incorporation of markers in the melt.[6] The molecular orientation depends on the normal stress differences, and it can be simulated by a Maxwellian-type model in stationary regime.[7] The second stresses are due to thermal stresses that appear during the cooling of the successive polymer layers due to the fact of incomplete thermal retractions.[8] They are influenced by a great number of parameters linked to the injection process, and they depend on the polymer elastic properties. Their variation versus the thickness is generally of parabolic shape with a compressive stress at the surface and a tensile stress at the center.[9] They are often superior to the flow stresses[1] on which they superimpose with values included between 1 and 10 MPa. The used calcula-

Correspondence to: J. Pabiot (lafranche@ensm.douai.fr).

Contract grant sponsor: RENAULT Directorate of Research.

Journal of Applied Polymer Science, Vol. 68, 1661–1669 (1998)

 CCC 0021-8995/98/101661-09

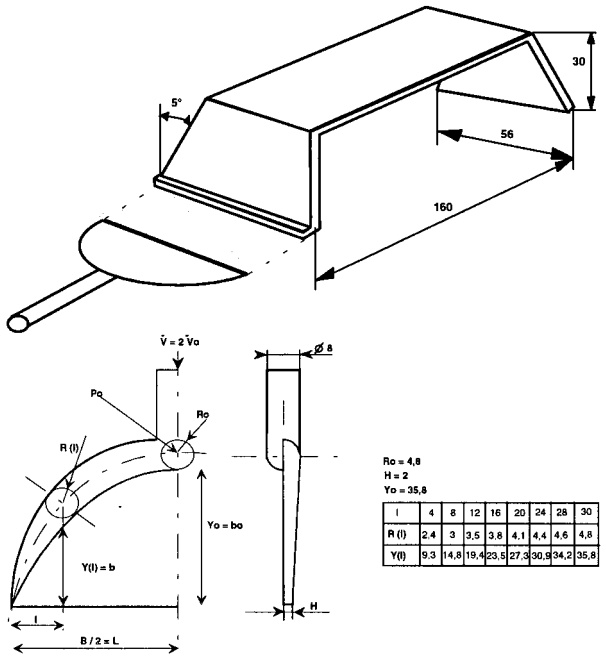

Figure 1 Schematic representation of plastic part and fill-type gate geometry.

tion models are derived from the ones employed in inorganic glass manufacturing.[10] Thermoelastic laws have been commonly used by the authors.[11,12]

The results of a study consisting in establishing relationships between the deformation of injected plastic parts and internal stresses have been presented here. The impact of the dissymmetry of the structure in thickness on deformation has been evaluated from the coupled effect of thermal stresses and the molecular orientation during a temperature variation.

EXPERIMENTAL STUDY

General Means

The injected plastic part is a 2-mm-thick box in a U shape. It is fed by a film type gate (Fig. 1). The material is an isotactic homopolymer of polypropylene. The injection-molding machine has a 2000 kN clamping force. Its essential particularity resides in the melt polymer pressure closed-loop control of the postfilling stage. In that case, the magnitude of entry of the regulation is not a hydraulic pressure as in most machines, but more directly melt pressure information from a sensor inside the cavity.[13]

The molding parameters are as follows: Injection speed: 20 mm/s; postfilling time: 10 s; average mold temperature: 50°C; average melt temperature: 230°C; cooling time: 5 s.

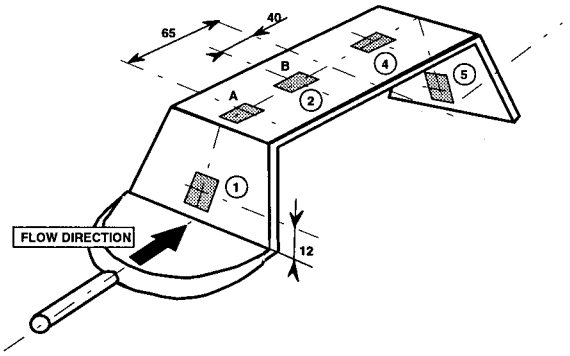

Figure 2 Sample localization for (1, 2, 4, 5) IR dichroism measurements and for (A,B) dilatometrical analysis of image (DAI).

Molecular Orientation Measurement

Molecular orientation is undertaken by the infrared dichroïsm method on microtome slices (10 mm $\times$ 6 mm $\times$ 20 μm) cut through thickness from samples, as shown in Figure 2. The measurement leads to the second moment of the global orientation function,[22,23] which allows separate orientation for both crystalline and amorphous phases of the polymer. The absorption bands were those generally employed for the polypropylene,[14] at 973 cm^{-1} for the pure amorphous phase and 998 cm^{-1} for the pure crystalline phase. The absorption of IR radiation for a chemical group in the chain depends on the angle α between the transition moment with the chain axis, and on the angle θ between the chain axis and orientation direction (Fig. 3).

The second-order moment of the orientation function $\langle P2 \cos \theta \rangle$ is linked to α and θ by[23]

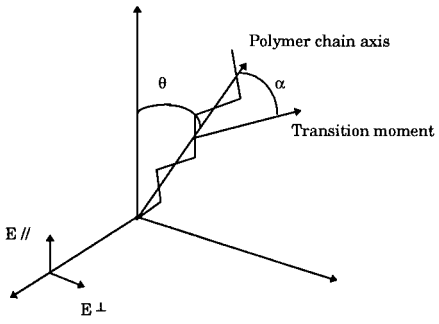

Figure 3 Definition of α and θ angles.[23]

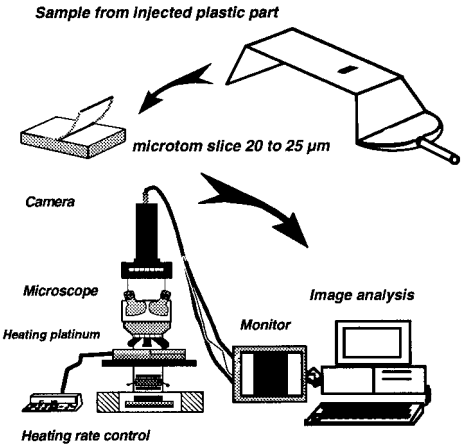

Figure 4 Measurement apparatus of thermal stresses by DAI.

$$\langle P2\cos\theta\rangle = \frac{3\langle\cos^2\theta\rangle - 1}{2} \qquad (1)$$

The orientation function varies from −0.5 (perfect perpendicular orientation) to 1 (perfect parallel orientation). FTIR spectra were obtained from a Fourier transform spectrophotometer. The microtome slices are fixed on a sample holder with a polarizer. The absorbance measurements are taken for each IR absorption band in a parallel and a perpendicular polarization with the flow direction. In this study, only the crystalline absorption band was inspected.

Thermal Stresses Measurement

A thermal expansion measurement method on microtome slices of 2 mm × 0.5 mm × 20 μm size, developed by Delbarre,[15] was used. The microtome slices were peeled off from samples of 10 × 6 mm size cut along the flow axis (Fig. 2). The slice is put between two coverglasses on a heating platinum under an optical microscope in transmission (Fig. 4). A TTL camera transmits the image to an image analyst of Visilog type. The processing is achieved on images of 512 × 512 pixels size, the sensitivity is about 1 pixel, giving a precision of 0.02% on the strain calculation. The heating rate is 5°C/min.

The slice thermal expansion is recorded versus temperature for two successive thermal treatments between 30 and 100°C. The shrinkage due to stress relaxation in the sample was noticed between the first and second treatment (Fig. 5). The strain ε achieved from the two treatments, after relaxation, makes it possible to access to the stress σ by an elastic law:

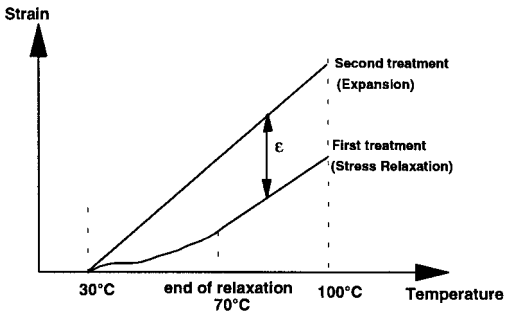

Figure 5 Principle of strain measurement due to thermal stresses.

$$\sigma = \frac{E}{1-\nu}\cdot\varepsilon \qquad (2)$$

where E is Young's modulus and ν the Poisson ratio. We consider a homogeneous material, and states of stress depend only on the temperature gradient in the thickness.

EXPERIMENTAL RESULTS

Measure of Orientation Field

The orientation profile from the measures versus thickness is similar to that found by many authors. It has four zones (Fig. 6):

- A first zone (1) where orientation increases due to shear stresses and Fountain flow ef-

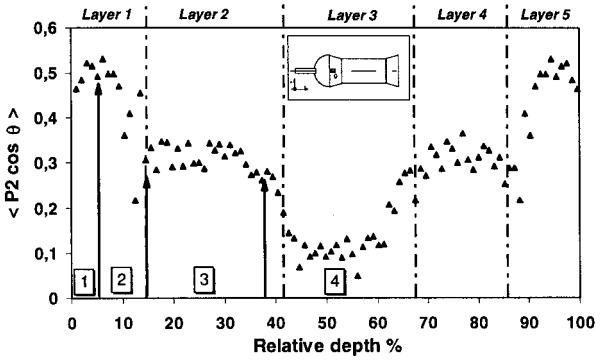

Figure 6 Molecular orientation of the crystalline phase (near the gate) from infrared measurements.

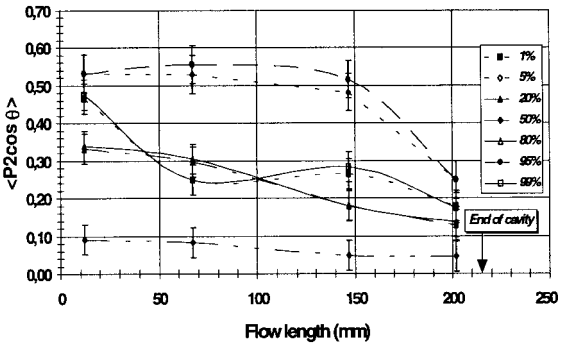

Figure 7 Molecular orientation study versus the flow length for 1, 5, 20, 50, 80, 95, and 99% in the thickness.

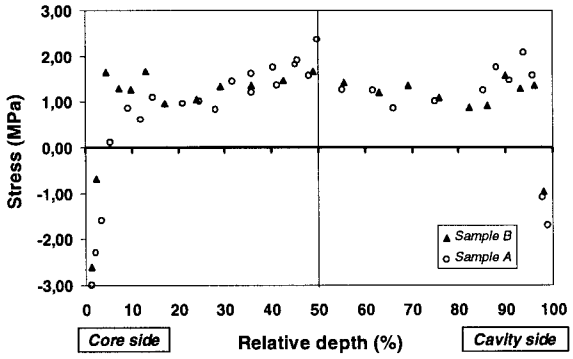

Figure 8 Thermal stress profile versus thickness.

fects from the filling stage of cavity (about 5% of the thickness).

- A second zone (2) where orientation decreases rapidly. This phenomenon is generally attributed to a quenched effect of packing pressure that displaces the crystallization isotherm to the center of the part (increase in crystallization temperature of 47°C for a variation of 100 MPa), by freezing the orientation during relaxation after the flow.[17]
- A third zone (3) where orientation increases due to the postfilling pressure.[16]
- A fourth zone (4) where relaxation is preponderant and orientation decreases rapidly to give an isotropic polymer.[25]

The evolution of molecular orientation following the flow axis (Fig. 7) shows that orientations of the postfilling zone (zone 3: 20 and 80%) decrease clearly, meaning an efficiency decrease for the transmission of pressure inside the part. The skin orientations (zone 1: 1 and 99%) decrease rapidly to reach a landing from a third of the filling course, which corresponds to a stabilization of flow rate. The underskin zone (zone 2: 5 and 95%) remains the same; we notice only a decrease at the end of filling where the edge effects induced by packing seem to influence a transversal orientation. The core zone presents a quasi constant orientation where the polymer does not show a particular organization and is therefore practically isotropic.

Measure of Thermal Stress Field

The relaxation control enables us to observe that it is effective between 50 and 70°C (Fig. 5). The temperature reference for stress calculation was fixed at 80°C. Young's modulus at this temperature is equal to 350 MPa, and the Poisson ratio[15] was fixed to 0.33.

Figure 8 shows the stress thermal profile that we obtained. We can notice compressive stresses in the skin and extensive stresses in the core with values evolving between −3 MPa and +2 MPa, which confirms printed evidence.[18] A stress dissymmetry between the two walls was observed with a lower compressive stress on the cavity side that leads to a dissymmetry in cooling. The parabolic profile, generally found in the literature on simulated calculations, does not appear in this case. Indeed, two stress peaks were noticed approximately at 10 and 90% of the thickness, whose origin can be attributed to polymer structural organization, due notably to the fact of molecular orientations, as some authors suggest.[16,17,19,25] This structural organization clearly appears on expansion measurements after whole stress relaxation (Fig. 9). A minimal thermal expansion was observed just under the skin, representative of a pronounced organization in the zone of great

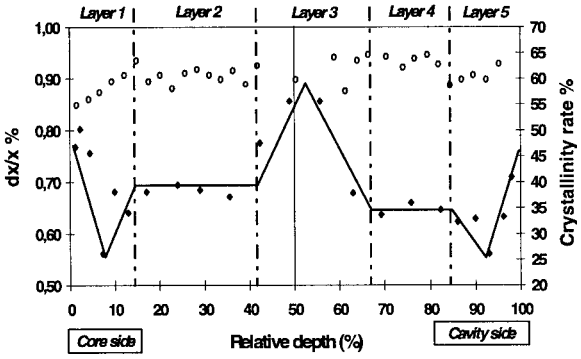

Figure 9 Thermal expansion profile at 80°C versus thickness from the second treatment (♦); crystallinity profile versus the thickness from DSC measurements (◇).

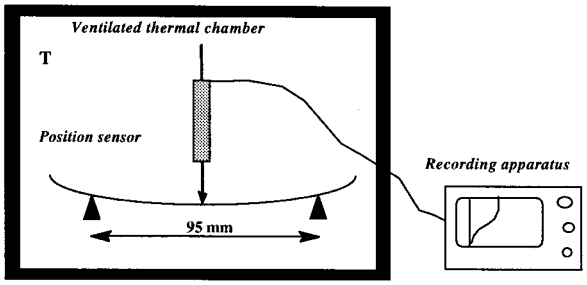

Figure 10 Experimental apparatus for deflection measurements versus temperature.

orientations (Fig. 6). A raised expansion appeared in the core where the polymer is isotropic. A dissymmetry of thermal expansion with regard to the average axis on the two landings of the curves was also noticed.

For morphologic consideration, the cristallinity rate was achieved from DSC measurements on microtom slices; the enthalpy value[24] of a 100% cristalline polymer was assumed at 150 J/g. The distribution on thickness does not allow us to bring a high gradient to the fore. We suppose, therefore, that only the orientation directs the expansion.

The thermal stress profile for a sample (A) placed at the junction of the superior plane of plastic part and the lateral flank (Fig. 2) shows a similar distribution to the first one (Fig. 8). A uniform stress distribution in the part has been admitted, at least in its symmetry plane.

DISCUSSION

Molecular orientation profiles and thermal expansion profiles versus thickness show that the injected part presents a comparable heterogeneous structure to the one of a multilayer composite.[25] After ejection, we can suppose that the deformation of the part comes from the coupled effect of thermal stresses and structural gradient versus thickness. On the other hand, if the composite has a dissymmetry of local properties with regard to the average plane of the part, a deformation directly linked to unit deformations of each layer with regard to their intrinsic properties was induced. Consequently, if a temperature variation is applied to the whole structure, it will act on the local deformations of each layer, and thus on the global deformation of the part.

The structural dissymmetry with regard to the average plane of the part was shown by our thermal expansion measurements (Fig. 9). The aptitude of the multilayer composite to reply to a thermal sollicitation was pointed out by a measure of deflection. The experimental apparatus is shown on Figure 10. The injected plastic part reduced to its main plane of 125 × 51 × 2 mm size is placed on two supports in a thermal chamber. The deflection was measured by a differential transformer position sensor placed to the axis of symmetry. The measure is in static form at temperatures of −20, 40, and 50°C (limit of temperature from which the stress relaxation starts).

The test shows that the temperature acts on the deflection of the sample. We notice variations of deflection between −7 and 10% compared to the one measured at 23°C (Fig. 11). From this experiment, we confirm that the composite structure plays a great part in the deformation.

The experimental measurements make it possible to confirm by calculation where we assimilate the plastic part as a composite of five elementary layers with the properties defined by their average orientation rate as (1) two skin layers, strongly oriented with great stiffness, of about 10% each of the total thickness; (2) one core layer, feely oriented with low stiffness, of 15 to 20% of the total thickness; and (3) two intermediate layers of mean orientation.

To make the calculation, we need to know the linear thermal expansion coefficient and Young's modulus of each elementary layer. In fact, we need to estimate the evolution of these parameters according to the molecular orientation.

Correlations between linear thermal expansion coefficient calculated between 30 and 80°C and the second-order coefficient of the orientation distribution $\langle P2 \cos \theta \rangle$ (Fig. 12) were established from superposition of thermal expansion curve (Fig. 9) and molecular orientation.

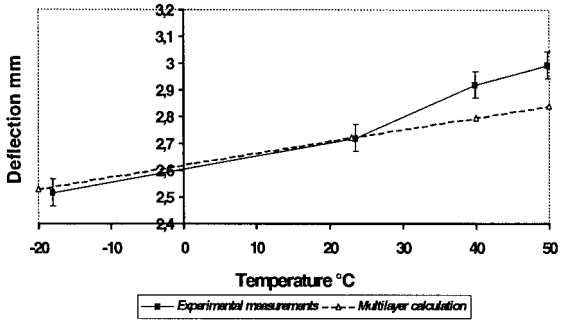

Figure 11 Evolution of deflection versus temperature: experimental results (full line), calculation (dashed line).

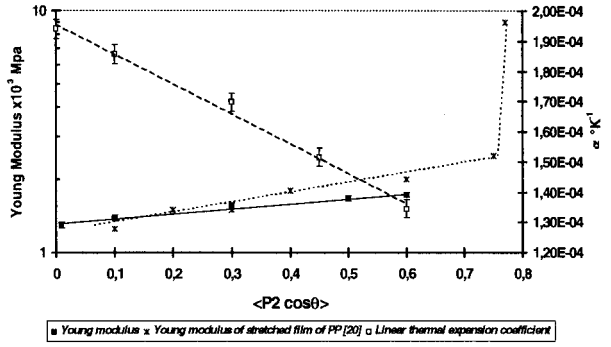

Figure 12 Evolution of Young's modulus and linear thermal expansion coefficient measured in orientation direction versus molecular orientation for the 3050MN1 PP: (--∗--) results from a stretched PP according to ref. 20.

To estimate Young's modulus, the local stiffnesses were measured from a three-point deflection test on specimens of 50 × 15 × 2 mm size cut off the plate. In fact, we have samples whose second-order coefficient of the orientation distribution $\langle P2 \cos \theta \rangle$ covers an orientation field of 0.1 to 0.6 according to their position on the part (Fig. 7). The 0.1 oriented core layer is easily characterized by cutting a sample at the end of cavity because it represents 80% of the total thickness. By buffing skin layers, we can directly access to the mechanical properties of the 0.1 orientation layer for a Young's modulus calculated in deflection of 1390 MPa. For the 0.3 orientation layer, we were interested in three-layer configurations by buffing the two skin layers. The global modulus achieved from deflection measurements enabled us to access to the modulus of each layer from a method of calculation used for the "sandwich" materials. Finally, for the 0.5 and 0.6 orientation layers, we used the previous results and the global modulus calculated from deflection tests on unbuffing samples. The evolution of Young's modulus calculated from deflection test versus $\langle P2 \cos \theta \rangle$ are shown in Figure 12. The values agree with the results achieved on uniaxial orientation of polypropylene films.[20]

From this data, the calculation hypotheses are as follow: (1) the polymer is considered to have an elastic behavior, (2) the modulus and linear thermal expansion coefficients were supposed constant for the temperature field of the calculation, (3) we suppose each layer is a homogeneous material, and (4) it has been admitted the initial state corresponds to the state of deformation at 23°C with a deflection of 2.72 mm.

The average axial stiffness of multilayer composite is then equal to the sum of stiffness of each element constituting it:

$$\bar{A}\bar{E} = \sum_{i=1}^{n} A_i E_i \tag{3}$$

with E as Young's modulus and A is cross-sectional area.

The change of dimension of multilayer composite during a temperature variation depends on the linear thermal expansion coefficient α by the relationship

$$\varepsilon^T = \alpha \cdot \Delta T \tag{4}$$

The free thermal strain ε^T can be associated with the stress by Hooke's law such as

$$\sigma^T = E \cdot \varepsilon^T \tag{5}$$

and

$$F^T = A \cdot E \cdot \varepsilon^T \tag{6}$$

The total equivalent thermal force F^T of the multilayer represents the sum of unit forces of each layer:

$$F^T = \sum_{i=1}^{n} F_i^T = \sum_{i=1}^{n} A_i E_i \alpha_i \Delta T \tag{7}$$

The global strain ε given by the ratio of F^T on axial stiffness:

$$\varepsilon = \frac{F^T}{\bar{A}\bar{E}} \tag{8}$$

From eqs. (3), (6), and (7), the global strain of multilayer is given by

$$\varepsilon = \frac{\Delta T \cdot \sum_{i=1}^{n} A_i E_i \alpha_i}{\sum_{i=1}^{n} A_i E_i} \tag{9}$$

The residual strain ε^R is produced by the global strain ε resulting from the excess of thermal strain of individual layers ε^T is

$$\varepsilon_i^R = \varepsilon - \varepsilon_i^T \tag{10}$$

which gives for the layer 1 of five layers of material

Table I Data for Calculation of Multilayer Composite

Layer	Young's Modulus (MPa) at 23°C	Thermal Expansion Coefficient ($°K^{-1}$)	Position from the Average Axis (m)	Cross-Section Area (m^2)
1	1730	1,120E-4	−0,883E-3	1,585E-5
2	1557	1,400E-4	−0,447E-3	2,859E-5
3	1350	1,740E-4	+0,072E-3	2,436E-5
4	1600	1,300E-4	+0,519E-3	2,120E-5
5	1730	1,120E-4	+0,883E-3	1,585E-5

$$\varepsilon_1^{\mathrm{R}} = \frac{\Delta T(A_2E_2(\alpha_2-\alpha_1) + A_3E_3(\alpha_3-\alpha_1) + A_4E_4(\alpha_4-\alpha_1))}{(A_1E_1 + A_2E_2 + A_3E_3 + A_4E_4)} \quad (11)$$

The corresponding residual stress is given by the relationship

$$\sigma_1^R = E_1\varepsilon_1^R \quad (12)$$

The calculation is achieved for each layer so we can deduce the total moment

$$M_T = \sum_{-y}^{+y} \sigma_i^R \cdot w \cdot \delta y \cdot y_i \quad (13)$$

The radius of curvature R and deflection f are then calculated from the following relationships:

$$R = \frac{EI_x}{M_T} = \frac{Ewh^3}{12M_T} \quad (14)$$

$$f = R\left[1 - \cos\left(\frac{L}{2R}\right)\right] \quad (15)$$

where h is the thickness of plate, w the width of plate, L the length of plate, I_x the moment of inertia, and E the average Young's modulus.

Data of calculation of deflection are presented in Table I.

The calculation shows a good correlation with experimental results (Fig. 11), a gap on deflection values calculated at temperatures of 40 and 50°C was noticed, this can be attributed to the second calculation hypothesis.

To point out the coupled effect of thermal stresses and stresses due to the multilayer structure, a thermal treatment of the part was carried out at a temperature of 100°C for 5 h to relax all the thermal stresses. This annealed temperature corresponds to the limit temperature beyond which a molecular orientation relaxation begins, together with a modification of crystalline morphology.[21]

The orientation profile obtained after thermal treatment shows that the orientation levels are not allocated (Fig. 13), the level of thermal stresses after annealed remains negligible in comparison with the initial profile (Fig. 14), and finally, the thermal expansion profile indicates that the material has undergone no major structural modification (Fig. 15).

The annealed part is placed in the experimental apparatus as described by Figure 10 to measure deflection versus temperature at −20, 40, and 50°C. We notice that thermal treatment de-

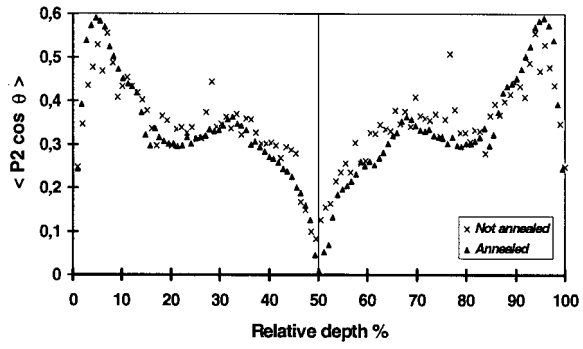

Figure 13 Effect of a thermal treatment on molecular orientation profile versus thickness.

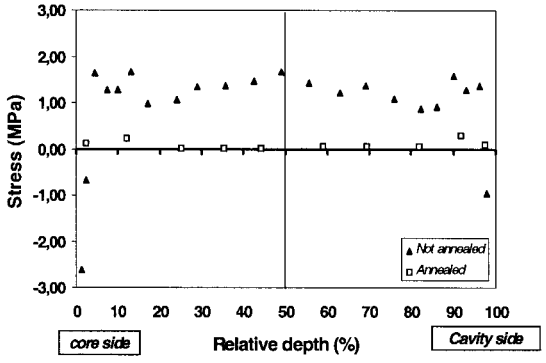

Figure 14 Thermal stress profile versus thickness: influence of a thermal treatment at 100°C.

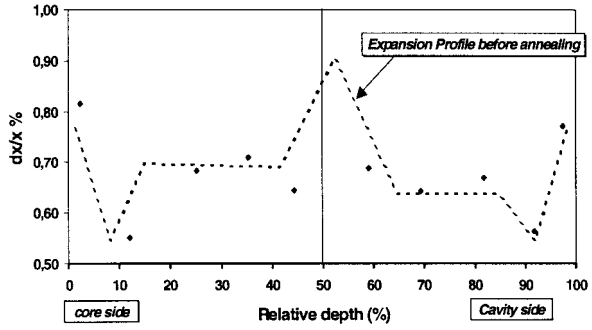

Figure 15 Expansion profile versus thickness: influence of a thermal treatment at 100°C.

creases the deflection value by 34% (Fig. 16). The multilayer structure of the polymer always reacts with a temperature variation. A similar deflection evolution with regard to the one recorded for the unannealed sample was also noticed.

We supposed that the total moment accountable for the initial deflection of the part can be interpreted as the algebric sum of the moment induced by the dissymmetric distribution of thermal stresses versus thickness (Fig. 8) and the one caused by the structural gradient as a result of molecular orientations is itself dissymmetric in regard to the average plane of the part:

$$M_T = M_S + M_{\sigma_r} \tag{16}$$

with M_T the total moment, M_s the moment due to the structure alone, and $M_{\sigma r}$ the moment due to thermal stresses alone.

Knowing the deflection value before and after annealing, we can access then to M_T and M_s by using relationships 14 and 15. From this data, the moment attributed to thermal stresses alone was deduced $M_{\sigma r}$ (0.017 N m). To validate these experimental results, the deflection can also be estimated directly from the curve of thermal stress distribution versus thickness obtained from measurements by dilatometrical analysis of image (DAI; see Fig. 17). The material was considered isotropic and homogeneous. The moment associated with the stress distribution is given by the relationship

$$M_x = \sum_{-y}^{+y} \sigma_i \cdot W \cdot \delta y \cdot y_i \tag{17}$$

where W is the width of plate.

The radii of curvature and the deflection are calculated by relationships 14 and 15, average Young's modulus E is 1300 MPa (modulus of isotropic material at 23°C). For a part of 51-mm width and 2.08-mm thickness, we obtain (1) a moment $M_x = 0.015$ N m in regard to a value of 0.017 N m for a experimental analysis; (2) a radius of curvature $R = 3.298$ m; and (3) a deflection $f = 0.85\ 10^{-3}$ m.

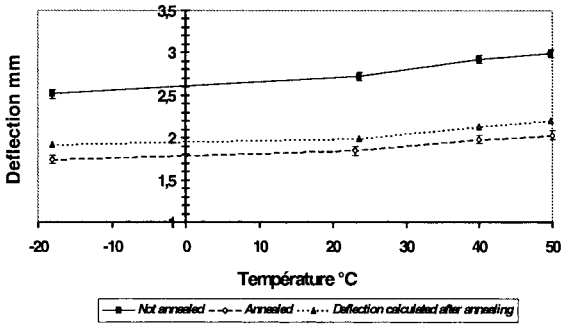

Figure 16 Influence of a thermal treatment on deflection, comparison between experimental results and calculation.

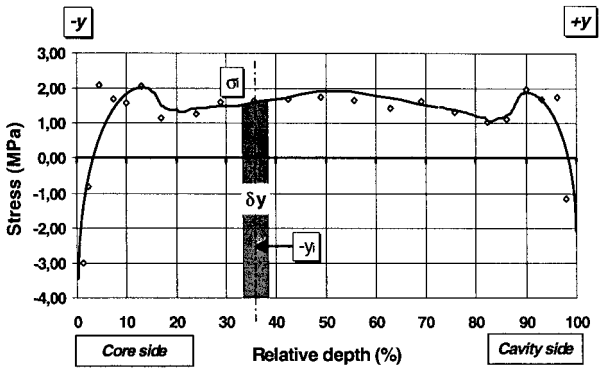

Figure 17 Representation of the calculation of the moment due to the thermal stress profile.

CONCLUSIONS

The study of molecular orientation distribution in an unidirectional flow has revealed the anisotropy and the heterogeneity of the part.

From local measurements of orientation by infrared dichroism and from internal thermal stresses measurements by DAI, correlations between orientation rates and local stiffnesses measured from deflection tests, on the one hand, and the linear thermal expansion coefficients, on the other hand, have been established. The data integrated in a deformation calculation of a part constituted as a multilayer composite material de-

fined by its dilatometric profile versus thickness, have brought to the fore the coupling of cooling stresses and those induced by structural gradient (orientations, crystallinity). Calculations have corroborated the deflection measurements made in the temperature where the effects have been separated by a thermal treatment of the part at a temperature of 100°C for 5 h to release all cooling stresses. The global deflection has, therefore, been expressed as the result of the superposition of the effects generated by thermal stresses whose dissymmetry induces a curvature, and the effects of a structural gradient itself dissymmetric, due to molecular orientations and crystallinity of the polymer, equally responsible for a deformation. A coupling between stresses due to the heterogeneous cooling and the structural organization of the part induced by the process (filling, packing, and postfilling stages) for molecular orientations and by the cooling rates for crystallinity, has thus been determined.

The authors would like to thank Renault Directorate of Research for their financial and technical support.

REFERENCES

1. A. I. Isayev and D. L. Crouthamel, *Polym. Plastic Technol. Eng.,* **22,** 137 (1984).
2. S. J. Willey and A. S. Ulmer, *ANTEC* (1986).
3. L. C. E. Struik, *Polym. Eng. Sci.,* **18,** 799 (1978).
4. W. Rose, *Nature,* **191,** 242 (1961).
5. Z. Tadmor, *J. Appl. Polym. Sci.,* **18,** 1753 (1974).
6. G. Gogos, C. F. Huang, and L. R. Schmidt, *Polym. Eng. Sci.,* **26,** 1457 (1986).
7. J. J. Pesce, Doctorial Theses, Université Louis Pasteur de Strasbourg, (1993).
8. G. Pötsch and W. Michaeli, *ANTEC,* 355 (1990).
9. J. Kubat and M. Rigdahl, *Polymer,* **16,** 925 (1975).
10. B. D. Aggarwala and E. Saibel, *Phys. Chem. Glasses,* **2,** 137 (1961).
11. G. Titomanlio, V. Drucato, and M. R. Kamal, *Int. Polym. Proc.,* **I,** 55 (1987).
12. K. M. B. Jansen, *Int. Polym. Proc.,* **IX,** 82 (1994).
13. P. Devos, F. Laurent, J. Pabiot, and M. Ryckebusch, *Polym. Proc. Soc.,* March 24–27 (1992).
14. H. Mavridis, A. N. Hrymak, and J. Vlachopoulos, *Polym. Eng. Sci.,* **26,** 449 (1986).
15. P. Delbarre, B. Jasse, J. Pabiot, and F. Rietsch, *J. Appl. Polym. Sci.,* **49,** 609 (1993).
16. G. Menges, H. Ries, and T. Wiegmann, *Kunstoffe,* **77,** 433 (1987).
17. J. P. Trotignon, *J. Appl. Polym. Sci.,* **34,** 1 (1987).
18. M. Thompson and J. R. White, *Polym. Eng. Sci.,* **24,** 227 (1984).
19. A. V. Iacopi and J. R. White, *J. Appl. Polym. Sci.,* **33.** 577 (1987).
20. M. F. Bottin, doctoral thesis, Université "Claude Bernard" de Lyon I (1979).
21. E. Lafranche, doctoral thesis, Université des Sciences et Techniques de Lille Flandres Artois (1996).
22. I. M. Ward, *J. Polym. Sci., Polym. Symp.,* **58,** 1 (1977).
23. R. J. Samuels, *Structured Polymer Properties,* Wiley, New York, 1974.
24. B. Wunderlich, *Macromolecular Physics,* Vol. 3, Academic Press, New York, 1980.
25. S. S. Katti and J. M. Schultz, *Polym. Eng. Sci.,* **22,** 1001 (1982).